Noise Performance of Time-Domain CMOS Image Sensors

Fernando de S. Campos, José Alfredo C. Ulson,
José Eduardo C. Castanho and Paulo R. Aguiar

Additional information is available at the end of the chapter

1. Introduction

Temporal noise is the main disadvantage of CMOS image sensors when compared to charged couple devices (CCDs) sensor. The typical 3T active pixel sensor (APS) architecture presents as main noise sources the photodiode shot noise, the reset transistor and follower thermal and shot noise, the amplifier thermal and 1/f noise, the column amplifier thermal and reset noise (Zheng, 2011; Brouk, 2010; Jung, 2005; Tian, 2001; Derli, 2000; Yadid-Pecht, 1997). In order to reduce the APS noise several approaches have been proposed in the literature. Some of these approaches are the use of high gain preamplifiers, correlated multiple sampling (CMS) and low bandwidth column-parallel single slope A/D converters (Sakakibara, 2005; Kawai, 2004; Suh, 2010; Lim, 2010; Yoshihara, 2006; Chen, 2012). However, APS in time domain has as advantage to show lower source of noise since it is composed only by a photodiode, a reset transistor and a voltage comparator. It shows as noise source only the reset transistor and the photodiode. Therefore, in principle, APS in time domain may presents lower overall noise.

The only two main noise source of APS in time domain are the reset noise and the integration noise. The source of reset noise is the incomplete reset operation. Tian et al. 2001, show that APS operates usually with incomplete reset operation. The incomplete reset operation originates a random reset voltage that varies from frame to frame as a source noise. It have been found that the reset noise is $kT/2C_{ph}$. During the integration period, the photodiode shot noise predominates generating a integration noise that is a function of the integration time, the photocurrent and the dark current. Altought the reset noise is the same to APS in voltage domain and in time domain, the integration noise must present different behavior in both approach. We show that while the integration time increases at higher photocurrents in

the voltage domain approach, the integration time is approximately constant at time domain approach. In this chapter the conventional frequency domain noise is not used. Instead, a temporal analysis is presented as proposed by (Tian, 2001).

2. CMOS active pixel sensor (APS) fundamentals

2.1. APS operation in voltage domain

Figure 1 shows a typical architecture of a conventional 3T CMOS active pixel. This pixel comprising a reset transistor M1, a source follower M2 and a line select transistor M3. When the line select is activated the select transistor is on and the source follower transmits the signal to the column bus keeping the photodiode isolated. After, the column signal at active load is amplified and converted to digital.
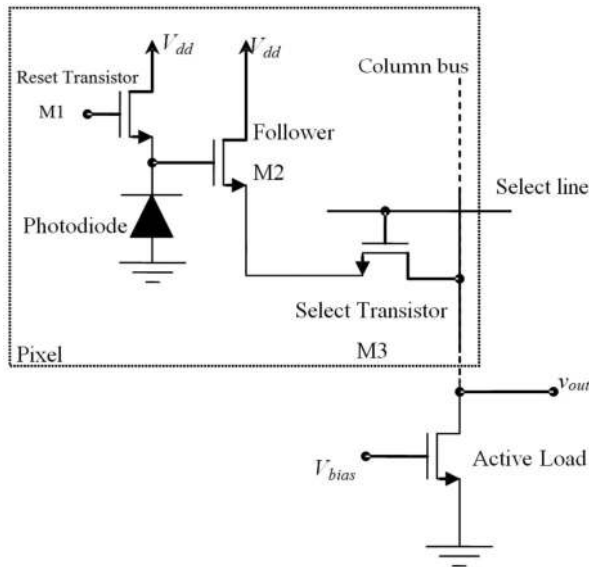
Figure 1. Diagram showing the conventional 3T APS architecture.

The conventional APS pixel of Figure 1 presents two operation stages: a reset period and a integration period (Figure 2). During reset period the reset transistor is on and the select transistor is off. In this period the photodiode is reversely charged to V_{dd}. After, the reset transistor is turned off initiating the integration period. In this period the photocurrent discharge the photodiode during an interval time called integration time. At the end of integration time the signal is readout externally by activation of select transistor.

The fixed-pattern noise (FPN) is the non-uniformity introduced in image due to parameters variation from pixel to pixel. It is one of main disadvantage of APS when compared to CCDs. In general, the FPN can be reduced by applying double sampled correlated (CDS). Figure 3 shows a simple circuit that can be used to implement CDS. The CDS operation is comprised by three steps; (1) sample and hold the reset signal, (2) sample and hold the signal after the integration time and (3) subtraction of signals of steps (1) and (2).
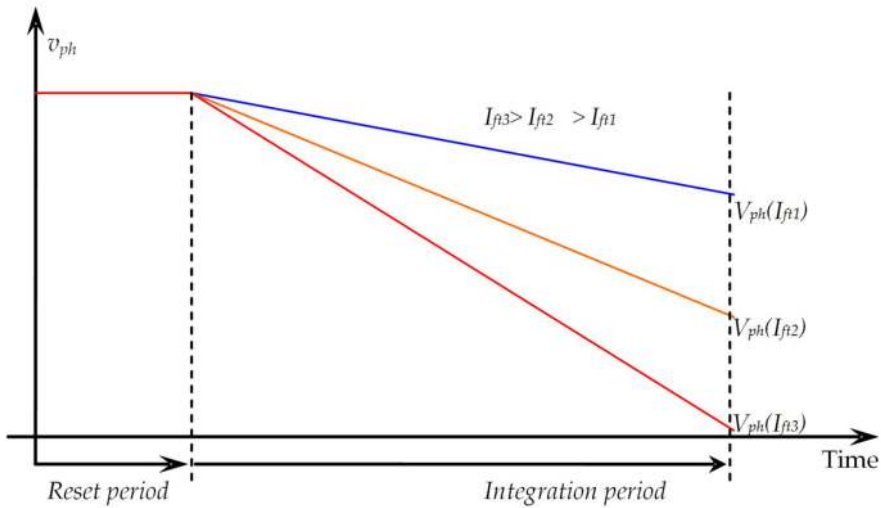

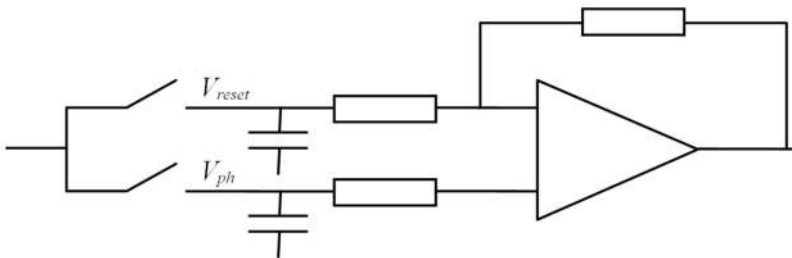**Figure 2.** APS operation in voltage domain.

Figure 3. Simple CDS circuit.

The photogate is another type of CMOS photodetector widely used (Fujimori, 2002; Sccherback, 2003; Mendis, 1997). The photogate is composed by a MOS capacitance, a pass transistor and a floating diffusion as shown in Figure 4 (Fossum, 1997). The photogeneration occurs in the depletion region of the MOS capacitor. The photogate operation can be separated into four stages (i) integration, (ii) the floating diffusion reset, (iii) transfer the load to the MOS

capacitor floating diffusion and (iv) reading of the floating node voltage signal. During the integration period, the terminal port (PG) of the MOS capacitance is set at V_{dd} and the carriers generated in the depletion region below the gate terminal (PG), are separated by the electric field junction metal-oxide-semiconductor. The polarization of the transfer terminal TX at low level isolates the load MOS capacitor node holding the floating charge under the gate region. The reset operation of the floating node consists on drive the transistor reset loading the floating node voltage V_{dd}. After resetting the floating node, the voltage of the transfer terminal TX is increased and the port terminal PG voltage MOS capacitor is reduced.
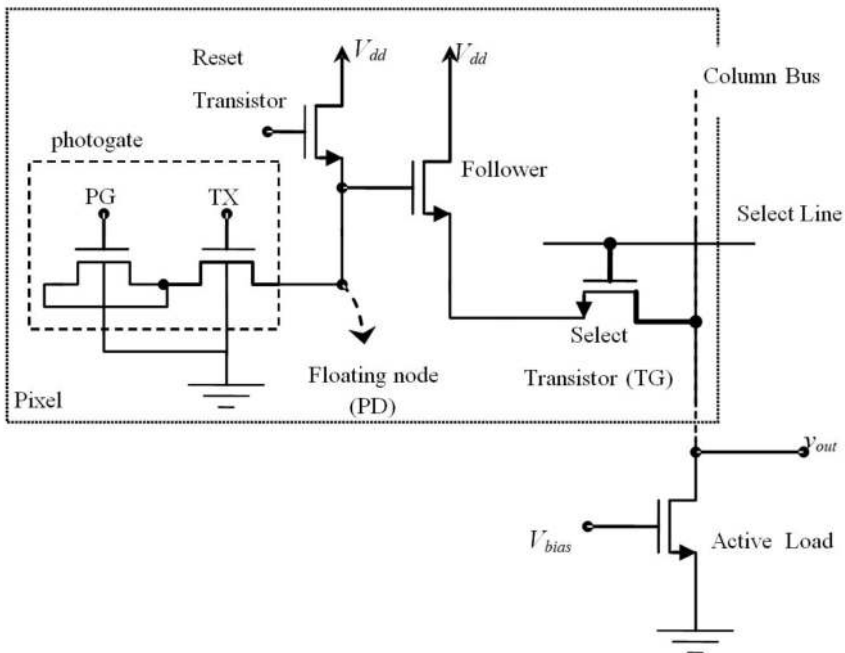
Figure 4. Active Pixel Photogate (PG-APS).

The charge transfer occurs with the polarization inversion of the TX and PG. The inversion of the potential resulting from PG and TX polarization cause displacement of charges stored in the region below the gate terminal (highest potential) toward the floating diffusion region (lower potential). After transfer, the transfer terminal voltage TX is reduced again isolating the MOS capacitor of the floating node FD and the loads are stored in the floating node. The new charge balance in FD leads to the floating node voltage variation that was initially charged with V_{dd}. The variation in voltage at node floating proportional to light intensity can be read externally. The main disadvantage of this photodetector is the lowest quantum efficiency, particularly in the blue region of the spectrum due to the reduction of the lumi-

nous flux caused by absorption of photons in the upper layer of polysilicon. In general, the circuitry for reading the signal APS systems with phototogate or photodiodes are the same or similar and in both cases are needed to readout the voltage of the photodetector.
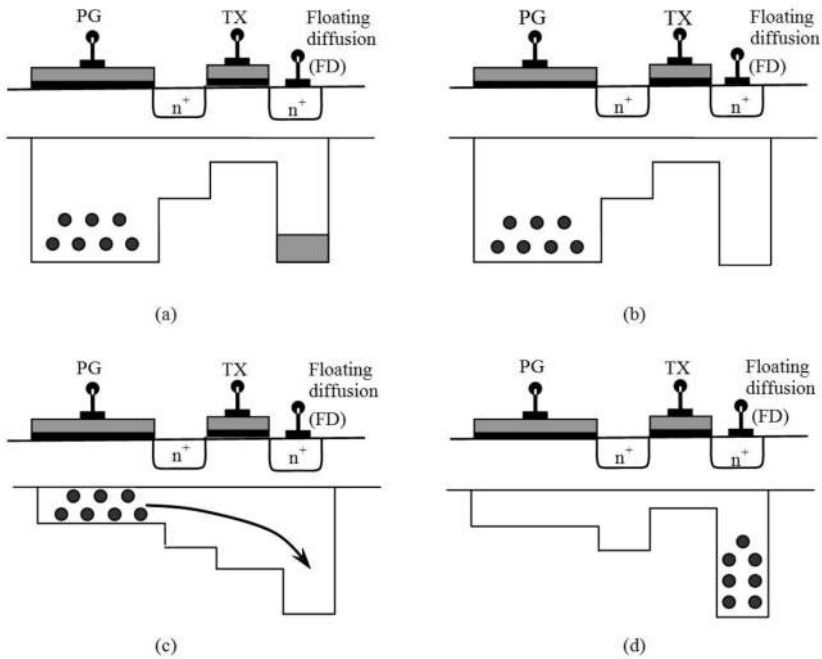
Figure 5. Photogate Operation Stages (potential diagram) (a) integration (b) *reset* (c) transfer (d) readout.

The logarithmic is another important type of CMOS Active Pixel (Figure 6). The logarithmic pixel is particularly attractive in applications that require image capture with high dynamic range (Kavadias, 2000; Joseph, 2002; Choubey, 2006). The logarithmic photoresponse allows you to capture light intensities in ranges of 6 orders of magnitude. However, the logarithmic pixel presents as disadvantages, high fixed pattern noise (FPN), low signal to noise ratio and a small swing of the output voltage. Furthermore, the logarithmic pixel requires long time to reach steady state at low light intensities. The pixel logarithmic is composed by a photodiode connected in series with a MOSFET (Figure 6). The output voltage reaches steady state when the MOSFET current becomes equal to the photocurrent ($I_D = I_{ph}$). The MOSFET operates in series and the gate and drain terminals connected directly ($V_{DS} = V_{GS}$) such that the given output voltage is given by $V_{out} = V_{dd}-V_{GS}$. Due to low values of photocurrent, the MOSFET operates in the weak inversion region in which the voltage is a logarithmic function of current. Therefore, the output voltage varies logarithmically with the luminous intensity.
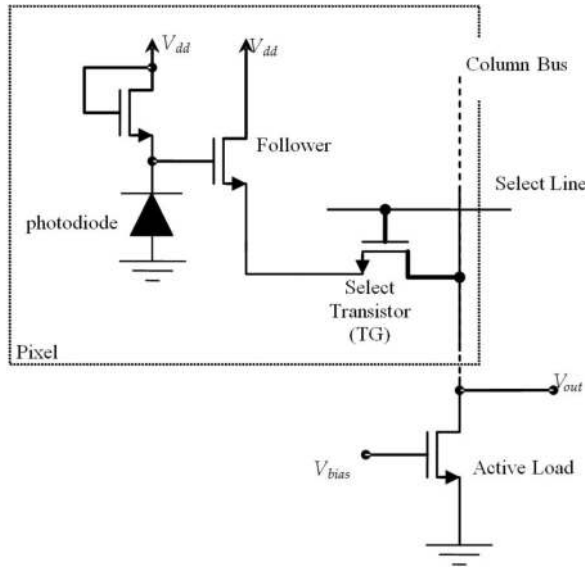
Figure 6. Logarithmic Active Pixel (LOG-APS).

2.2. APS Operation in time domain

Figure 4 shows the architecture of a typical CMOS APS which operates in the time domain. The pixel comprises a photodiode, a reset transistor, a voltage comparator and an 8-bit counter. The operation of the photodiode two basic steps, and integration reset as shown in Figure 5. In the time domain the incident light intensity is related to the time of discharge of the photodiode. The voltage of the photodiode during the integration period is compared with a reference voltage for measuring the time of discharge voltage of the photodiode. At the time the photodiode voltage falls below the reference voltage the counter count for storing the time the voltage of the photodiode lead to vary from the V_{dd} to the reference voltage V_{ref}
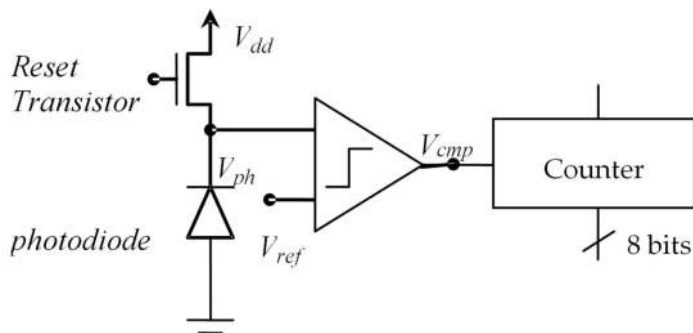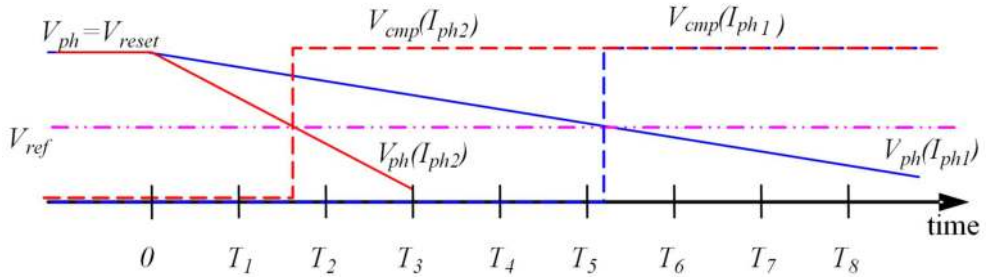

Figure 7. Typical APS architecture operating in time domain.

Figure 8. Main waveforms of APS operating in time domain.

The disadvantage of the APS operating in the time domain is the low fill factor. The fill factor is low due to the integration of the voltage comparator of the 8 bits counter per pixel. Alternatively to the low fill factor APS operating in the time domain in Figure 7, Fields et. al. proposed the method of reading multisampling in the time domain (Campos, 2008). Figure 9 shows a typical architecture of an APS multisampling operating in the time domain. The reading method consists in sampling the comparison result at time intervals. This method makes it possible to integrate the comparatorand the counter by column and therefore outside the pixel, reducing the number of integrated transistors per pixel and increasing the fill factor significantly.
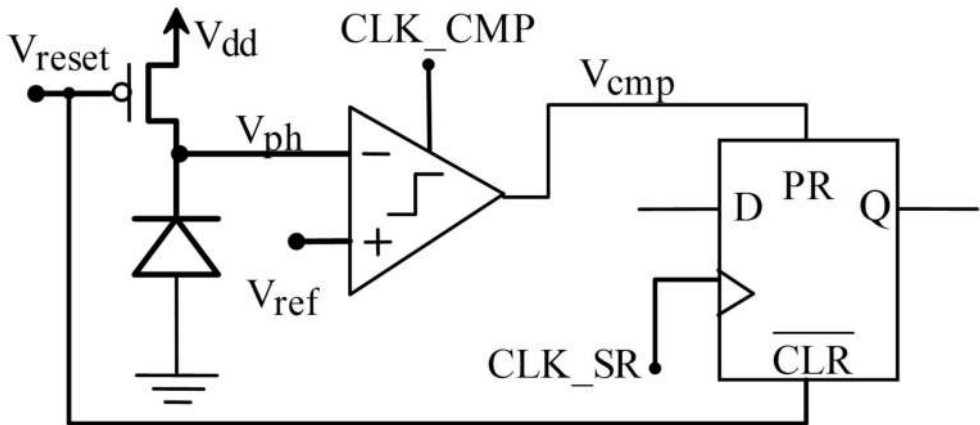
Figure 9. Typical APS multi-sampled in time-domain architecture.

3. Temporal noise

In this section we present the temporal noise analysis proposed by (Tian, 2001). Only the noise sources presented in time-domain APS are showed: the reset noise, and integration noise. During the reset period the charge time of photodiode is usually greater than the period. Also, the charge time in the reset period is a function of light intensity incident. Therefore, the voltage at end of reset period and beginning of integration time varies generating a random variation of voltage measured. This variation is known as reset noise. According Tian et al, the quadratic mean voltage of reset noise is given by

$$\overline{V_n^2} \cong \frac{kT}{2C_{ph}} \tag{1}$$

where k is the Boltzmann constant, T is the temperature in Kelvin and C_{ph} is the photodiode capacitance. Figure 10 shows the RMS reset noise voltage as a function of the photodiode capacitance at T=300K. For capacitances from 20fF to 100fF the RMS reset noise voltage is about a few hundred of milivolts.
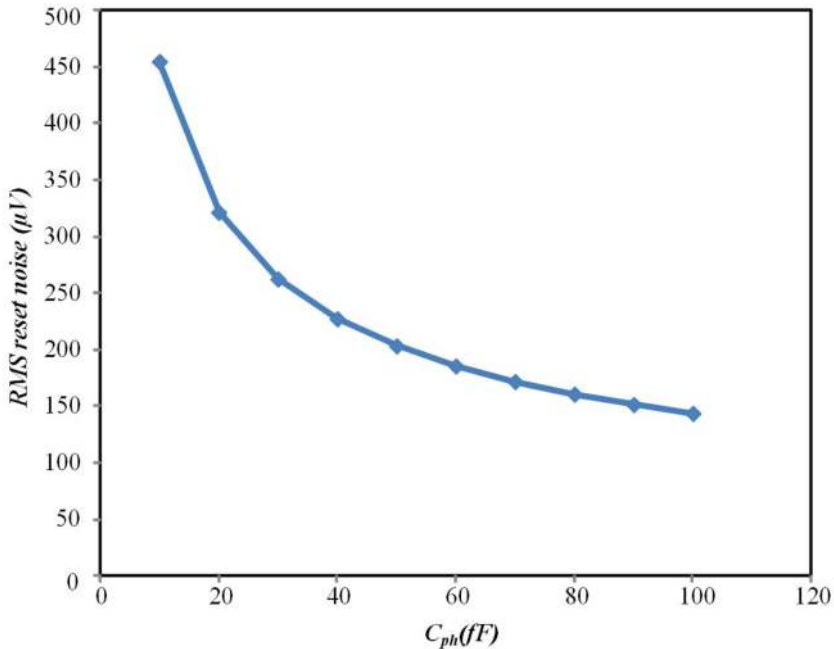

Figure 10. RMS reset noise voltage.

During the integration period the integration noise is composed by the shot noise related to the photocurrent and dark current. The quadratic mean voltage of the integration noise is given by

$$\overline{V_n^2(t_{int})} = \frac{q(i_{ph} + i_{dark})}{C_{ph}^2(v_{ph}(0))} t_{int} \left(1 - \frac{1}{2(v_{ph}(0) + \phi)} \frac{(i_{ph} + i_{dark})}{C_{ph}(v_{ph}(0))} t_{int}\right)^2 \tag{2}$$

where q is the elementary charge, i_{ph} is the photocurrent, i_{dark} is the dark current, v_{ph} is the photodiode voltage at integration time beginning, C_{ph} is the photodiode capacitance and t_{int} is the integration time (Tian, 2001). Figure 11 shows the RMS integration noise voltage considering C_{ph}=30pF, i_{dark}=2fF, $v_{ph}(0)$=3V and t_{int}=30ms. The RMS voltage integration noise is about a few milivolts for photocurrents in the range of 0.1pA to 1pA.
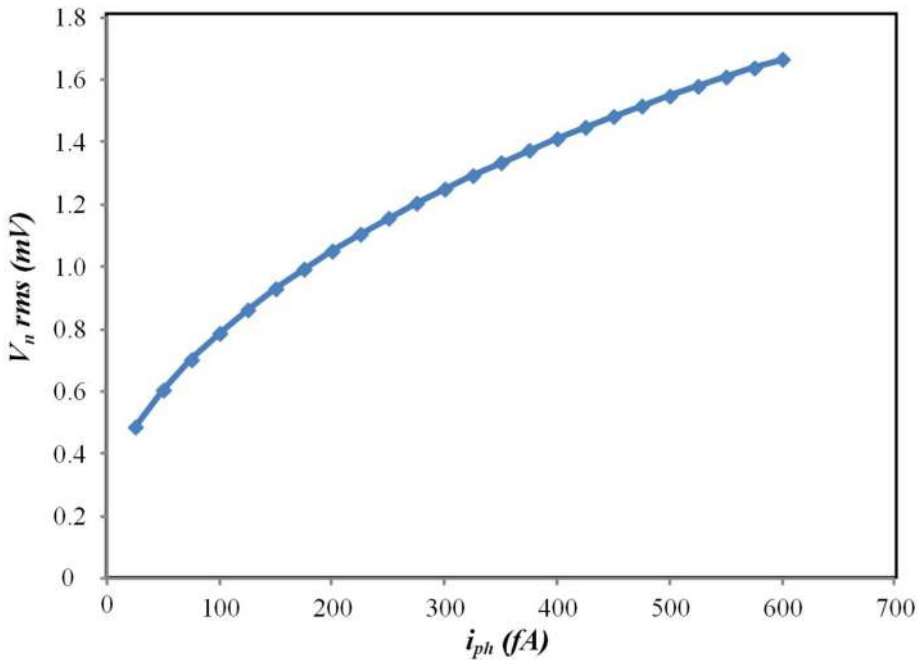
Figure 11. RMS integration voltage noise.

For APS operating in voltage domain, the follower transistor and select transistor of conventional APS also contributes to the total noise in APS, however, they are not presented in APS operating in time-domain and will be ignored in this analysis.

4. Temporal noise in time domain

As the APS in time domain pixel architecture is composed by a transistor reset, a voltage comparator and the photodiode, the main sources of noise are the reset noise and the integration noise as described in the last subsection. The reset operation of APS time domain is the same that the reset operation of APS voltage domain and, thus, the reset noise in time is the same given by equation (3). However, the integration time is different in time domain since the integration time is different for different values of photocurrent (see eq. (2) and (4)). Substituting eq. (2) in eq. (4), the integration noise in time domain is given by

$$\overline{V}_n^2 = \frac{q(i_{ph} + i_{dark})}{C_{ph}(v_{ph}(0))}\left(\frac{(v_{ph}(0) - v_{ref})}{i_{ph}}\right)\left(1 - \frac{1}{2}\frac{(i_{ph} + i_{dark})}{(v_{ph}(0) + \phi)}\left(\frac{(v_{ph}(0) - v_{ref})}{i_{ph}}\right)\right)^2 \qquad (3)$$

Figure 12 shows the integration noise voltage given by eq. 5 assuming V_{ref}=1.5V the same values of Fig. 11. As one can see the integration noise is approximately constant for $i_{ph} \gg i_{dark}$ and it is a V_{ref} function where the RMS integration voltage noise decreases as the reference voltage increases.
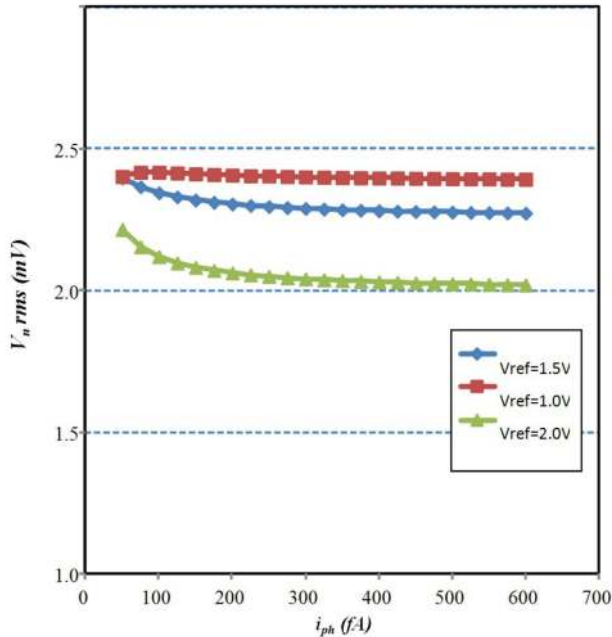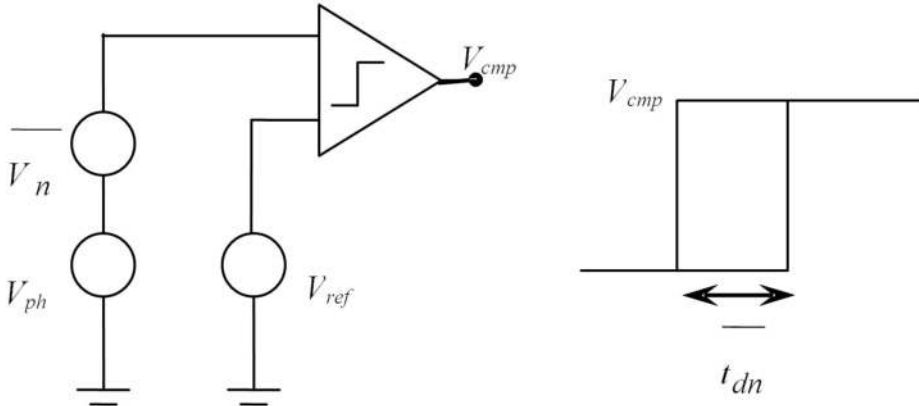

Figure 12. RMS integration voltage noise for APS operating in time-domain.

The voltage noise must reflect in a time noise on the comparison time given by equation (2). Assuming the equivalent circuit of Figure 10, the comparison time given by eq. (2) can be written as

$$t_d \cong \frac{\left(V_{reset} - V_{ref} + \overline{V_n}\right)}{i_{ph}} C_{ph}\left(v_{ph}(0)\right) \tag{4}$$

Figure 13. Noise in time-domain.

Manipulating equation (6) the discharge time with noise can be written as

$$t_d \cong T_d + \overline{t_{dn}} = \frac{\left(V_{reset} - V_{ref}\right)}{i_{ph}} C_{ph}\left(v_{ph}(0)\right) + \frac{\overline{V_n}}{i_{ph}} C_{ph}\left(v_{ph}(0)\right) \tag{5}$$

where T_d is the discharge time without noise and t_{dn} is the noise in time. However the signal-to-noise (SNR) ratio in time domain can be defined as

$$SNR_{time} = \frac{T_d}{\overline{t_{dn}}} = \frac{\left(V_{reset} - V_{ref}\right)}{\overline{V_n}} \tag{6}$$

Figure 14 shows the SNR_{time} assuming V_{reset}=3Vfor the three cases of Figure 12. The SNR drops at lower photocurrents values while it keeps constant at higher photocurrent values. Also, it is possible to note that the SNR values increase slightly as the reference voltage in-creases. However, one can note that for low reference value as at V_{ref}= 1.0V, the SNR is ap-proximately constant for over the photocurrent range.

5. Experimental Results

In this section the results of experiments show the behavior of noise in a multi-sampled time-domain APS proposed by (Campos, 2008). A pixel as shown in Figure 9 was implemented in 0.35μm AMS technology. The measurements were performed using an illuminator (Spectra Physics, with 100W Xenon lamp), optical filters and an integration sphere in a dark room. Figure 15 shows the measurement result for the characteristic discharge time versus illumination intensity, using a constant voltage of V_{ref}=1.5V. The analysis of slope in Figure 15 showed that the pixel sensitivity is about 3.4V-cm^2/s-W.
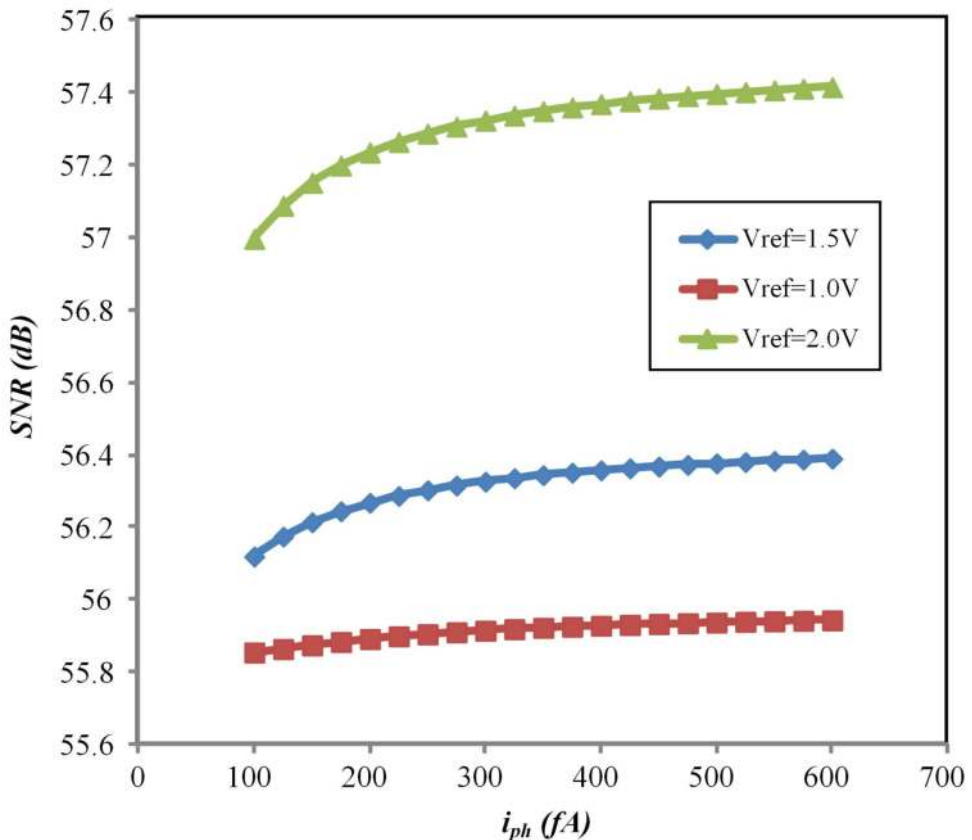
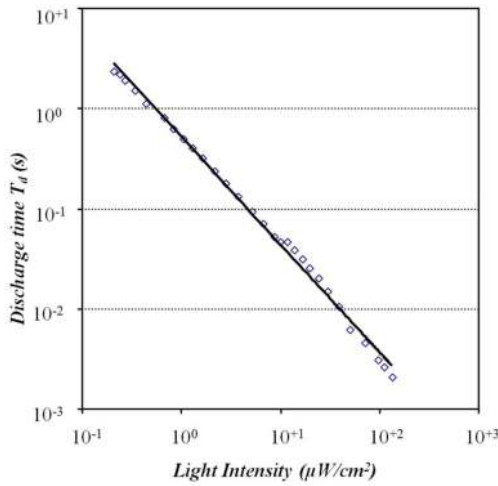**Figure 14.** SNR for APS operating in time-domain.

Figure 15. Discharge time.

Figure 16 shows the SNR as a function of light intensity obtained from the standard deviation and the medium comparison time obtained from the measurements at V_{ref}=1.5V. As expected from theoretical results, the SNR is approximately constant during 3 decades. It presents a SNR average of 54dB while the theoretical results is about 56dB. The SNR drops observed at high light intensities (>10^{+4}W/cm^2) may be related to the slew-rate of comparator that limits its performance at higher frequency operation. However, a better measurement procedure must be developed to caracterize the reference voltage effects and the comparator noise contribuition.
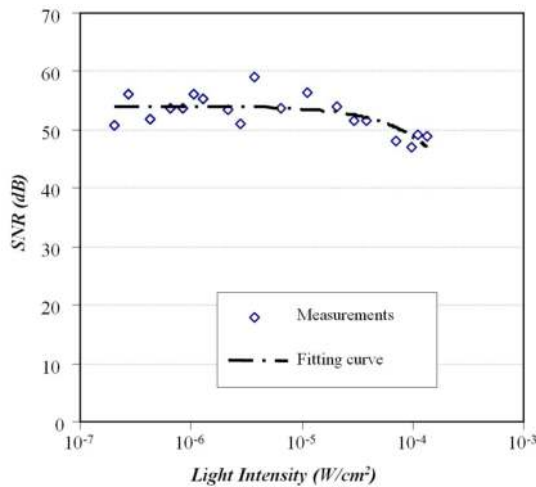

Figure 16. SNR in a time domain APS

6. Conclusions

The temporal noise analysis of APS in time domain was presented. Theoretical noise analysis indicated that the noise is constant when APS operates in time domain. The SNR is approximately constant when APS operates in time domain while the literature indicates that the SNR of APS operating in voltage domain drops at lower light intensities. Therefore, the results indicate that the operation in time domain is more suitable for low noise applications. Experimental results are in agreement with theoretical analysis.

Author details

Fernando de S. Campos[*], José Alfredo C. Ulson, José Eduardo C. Castanho and
Paulo R. Aguiar

*Address all correspondence to: fcampos@feb.unesp.br

Univ. Estadual Paulista "Júlio de Mesquita Filho" (UNESP) – Bauru campus, Brazil

References

[1] Brouk, I., Nemirovisky, A., Alameh, K., & Nemirovsky, Y. (2010). Analysis of noise in CMOS image sensor based on a unified time-dependent approach. *Journal Solid-State Electronics*, Elsevier, 54(1), 28-36.

[2] Campos, F. S., Marinov, O., Faramarzpour, N., Saffih, F., Deen, M. J., & Swart, J. W. (2008). A multisampling time-domain CMOS imager with synchronous readout circuit. *Analog Integrated Circuits and Signal Processing Journal*, 57, 151-159.

[3] Choubey, B., Aoyama, S., Otim, S., Joseph, D., & Collins, S. (2006). An Electronic-Calibration Scheme for Logarithmic CMOS Pixels. *IEEE Sensors Journal*, 6(4), 950-956.

[4] Chen, Y., Xu, Y., Mierop, A. J., & Theuwissen, A. J. P. (2012). Column-Parallel digital correlated multiple sampling for low-noise CMOS image sensors. *IEEE Sensors Journal*, 12(4), 793-799.

[5] Derli, Y., Lavernhe, F., Magnan, P., & Farre, J. A. (2000). Analysis and reduction of signal readout circuitry temporal noise in CMOS image sensors for low-light levels. *IEEE Transactions on Electron Devices*, 47(5), 949-962.

[6] Fossum, E. R. (1997). CMOS Image Sensors: Electronic Camera-On-a-Chip. *IEEE Transactions on Electron Devices*, 44(10), 1689-1698.

[7] Fujimori, I. L., Ching-Chun, W., & Sodini, C. G. (2002). A 256x256 CMOS Differential Passive Pixel Imager with FPN Reduction Techniques. *IEEE Journal of Solid-State Circuits*, 35(12), 2031-2037.

[8] Kavadias, S., Diericks, B., Scheffer, D., Alaerts, A., Uwaerts, D., & Bogaerts, J. (2000). A Logarithmic Response CMOS Image Sensor with On-Chip Calibration. *IEEE Journal of Solid-State Circuits*, 35(8), 1146-1152.

[9] Kawai, N., & Kawahito, S. (2004). Noise analysis of high-gain low-noise column read-out circuits for CMOS image sensors. *IEEE Transactions on Electron Devices*, 51(2), 185-194.

[10] Mendis, S. K., Kemeny, S. E., Gee, R. C., Pain, B., Staller, C. O., Kim, Q., & Fossum, E. R. (1997). CMOS Active Pixel Image Sensors for Highly Integrated Imaging Systems. *IEEE Journal of Solid-State Circuits*, 32(2), 187-197.

[11] Joseph, D., & Collins, S. (2002). Modeling, Calibration, and Correction of Nonlinear Illumination-Dependent Fixed Pattern Noise in Logarithmic CMOS Image Sensor. *IEEE Transactions on Instrumentation and Measurements*, 51(5), 996-1001.

[12] Jung, C., Izadi, M. H., La Haye, M. L., Chapman, G. H., & Karim, K. S. (2005). Noise analysis of fault tolerant active pixel sensors. *In proceedings of the 20th IEEE International Symposium on Defect and Fault Tolerance in VLSI Systems*, 140-148.

[13] Lim, Y., Koh, K., Kim, K., Yang, H., Kim, J., Jeong, Y., Lee, S., Lee, H., Lim, S-H., Han, Y., Kim, J., Yung, J., Ham, S., & Lee, Y-T. (2010). A 1.1e$^-$ temporal noise 1/3.2 inch 8 Mpixel CMOS image sensor using pseudo-multiple sampling. *In proceedings of International Solid-State Circuits Conference*, (San Francisco, CA, February), 396-397.

[14] Sakakibara, M., Kawahito, S., Handoko, D., Nakamura, N., Satoh, H., Higashi, M., Mabuchi, K., & Sumi, H. (2005). A high-sensitivity CMOS image sensor with gain-adaptive column amplifiers. *IEEE Journal of Solid State Circuits*, 50(5), 1147-1156.

[15] Sccherback, I., & Yadid-Pecht, O. (2003). Photoresponse Analysis and Pixel Shape Optimization for CMOS active pixel Sensors. *IEEE Transactions on Electron Devices*, 50(1), 12-18.

[16] Suh, S., Itoh, S., Aoyama, S., & Kawahito, S. (2010). Column-parallel correlated multiple sampling circuits for CMOS image sensors and their noise reduction effects. *Sensors*, 10, 9139-9154.

[17] Tian, H., Fowler, B., & El Gammal, A. (2001). Analysis of temporal noise in CMOS photodiode active pixel sensor. *IEEE Journal of Solid-State Circuits*, 36(1), 92-101.

[18] Yadid-Pecht, O., Mansoorian, B., Fossum, E., & Pain, B. (1997). Optimization of noise and responsivity in CMOS active pixel sensors for detection of ultra low light levels. *In Proceedings of SPIE*, (San Jose, CA, February 25), 3019, 125-136.

[19] Yoshihara, S., et al. (2006). A 1/1.8-inch 6.4 Mpixel 60 frames/s CMOS image sensor with seamless mode change. *IEEE Journal of Solid-State Circuits*, 41(12), 2998-3006.

[20] Zheng, R., Wei, T., Gao, D., Zheng, Y., Li, F., & Zeng, H. (2011). Temporal noise analysis and optimizing techniques for 4T pinned photodiode active pixel. *In proceedings of IEEE International Conference on Signal Processing, Communications and Computing (ICSPCC)*, 1-5.